APPENDIX B. SELECTION STUDY REPORT

TABLE OF CONTENTS

LIST OF TABLES

LIST OF FIGURES

1.0 INTRODUCTION

This report documents the Selection Study completed during Phase II of National Cooperative Highway Research Program (NCHRP) Project 9-36, *Improved Procedure for Laboratory Aging of Asphalt Binders in Pavements*. The Selection Study was included in Phase II of Project 9-36 to select either the Modified German Rotating Flask (MGRF) or the Stirred Air Flow Test (SAFT) for further development during the remainder of the project. As documented in the Interim Report, the literature review and review of research in progress conducted during Phase I concluded that both of these tests are promising approaches for an improved short-term aging procedure to be used in the United States with AASHTO M320, *Performance Graded Asphalt Binder*. The equipment required for both tests is relatively inexpensive, and they are easy to perform, applicable to both neat and modified binders, and reasonably reproduce the level of aging that occurs in AASHTO T240 *Effect of Heat and Air on a Moving Film of Asphalt (Rolling Thin Film Oven Test),* (RTFOT). The major issue unresolved through the Phase I literature review and review of research in progress was which of these two tests is best suited to extension to long-term aging. Only limited data was available on a long-term version of the German Rotating Flask, and no long-term aging data was available for the SAFT. The Selection Study documented in this report was designed to investigate the feasibility of extending these tests to long-term aging. Since cost, complexity, and ability to simulate the RTFOT were judged to be similar for the two tests, the extendibility to long-term aging became an important factor in selecting the short-term test method to be further developed in Project 9-36.

This report includes six sections in addition to this brief introduction. Section 2 discusses the aging conditions that were considered appropriate for a long-term aging test. The approach and materials used in the Selection Study are presented in Section 3. Sections 4 and 5 describe the laboratory testing and analysis that was included in the Selection Study. Section 4 presents various modifications to the MGRF and the SAFT that were made while attempting to develop prototype long-term versions of these tests, and compares the degree of aging in each to that obtained in AASHTO R28, *Accelerated Aging of Asphalt Binder Using a Pressurized Aging Vessel (PAV),* (PAV). Section 5 presents the results of a formal experiment addressing the effect

of viscosity on the degree of aging, a critical factor in the development of a long-term aging test. Finally, Section 6 presents conclusions and recommendations drawn from the Selection Study.

2.0 SELECTED LABORATORY CONDITIONS FOR SIMULATING LONG-TERM AGING

2.1 Temperature

The aging of asphalt binders, whether in the field or during accelerated laboratory aging, is a very complex process that has received considerable attention by researchers for many years. Previous studies indicate that the long-term aging mechanism is more reliably simulated when the accelerated aging is conducted as close as possible to the service temperature. Research conducted during the Strategic Highway Research Program (SHRP) clearly demonstrated that the aging mechanisms that occur in the laboratory during simulated aging change significantly when the aging temperature rises above approximately 110° C. Based on this past research, a temperature of 100 °C was used in the Selection Study.

2.2 Atmosphere

Pure oxygen, high pressure, and the combination of these have been used in the past to accelerate the aging process in long-term laboratory aging tests. For safety reasons, pure oxygen should not be used in tests intended for non-research testing laboratories. Additionally, some researchers have questioned the use of high air pressure to accelerate the aging process. Therefore, for the Selection Study, air at atmospheric pressure was used.

2.3 Duration

The long-term aging must be accelerated by some means in order to meet the needs of both the producers and users of the asphalt binder. Currently both pressure and temperature are used to accelerate the aging process in the PAV, resulting in a 20-hour test. During SHRP, a 144-hour test conducted at 60° C was proposed. Industry strongly objected to this protocol and consequently, the aging temperature was increased to 100° C. Based on discussions at the October 28, 2003 panel meeting, a maximum duration of 48 hours was used in the Selection Study to simulate long-term aging.

2.4 Quantity

Sufficient material must be available for characterizing the physical properties of the asphalt binder after long-term aging. Additionally, it may be desirable in the future to obtain samples at various times during the long-term aging to quantify aging rates. For grading according to AASHTO MP1a, at least 140 g of long-term oven aged binder should be available. The current procedures for the MGRF and the SAFT use 200 and 250 g of binder, respectively for the short-term aging test. After removal of a sample for short-term aged dynamic shear rheometer (DSR) testing, these sizes provide sufficient material for testing after long-term aging and for removing DSR samples for characterizing aging rates if desired. Sample sizes of 200 g for the MGRF and 250 g for the SAFT were, therefore, used in the Selection Study.

Table 1 presents a summary of the conditions selected by the research team for developing prototype versions of long-term aging tests based on the MGRF and the SAFT.

Table 1. Summary of Conditions for the Selection Study.

Condition	Value
Temperature	100 °C max
Atmosphere	Air at atmospheric pressure
Duration	< 48 hours
Quantity	Per current short-term testing protocol
Degree of Aging	Approximate PAV aging

3.0 EXPERIMENTAL APPROACH AND MATERIALS

3.1 Approach

The Selection Study was conducted in two parts. The first part of the study was an assessment of various modifications that could easily be made to the MGRF and the SAFT to produce prototype long-term versions of these tests. The goal in this effort was to obtain approximately the same degree of aging that occurs in the PAV subject to the constraints on temperature, atmosphere, and time given in Table 1. The binders used in this part of the study were a neat PG 58-28, a styrene-butadiene-styrene (SBS) modified PG 82-22, and a low density polyethylene (LDPE) modified PG 76-22. Table 2 presents the test conditions that were varied during this first part of the Selection Study. Section 4 presents a detailed discussion of the conditions investigated for each procedure.

Table 2. Summary of Conditions Investigated During the Selection Study.

Test	Conditions Investigated
MGRF	Morton versus smooth flask Rotational speed Mixing enhancers Scrapers
SAFT	Impeller type Position of air supply Rotational speed of impeller

The suitability of each of the various configurations was assessed based on:

- The degree of aging obtained relative to the PAV for the PG 58-28 and the PG 82-22.
- Visual assessment of the degree of mixing during the test.
- Visual assessment of separation for the two polymer modified binders.
- Potential for implementation as a specification test.

The second part of the Selection Study was a formal experiment designed to address whether the degree of aging in the prototype long-term versions of the tests is affected by the large differences in viscosities for neat and modified binders at the selected aging temperature of 100 °C. To emphasize the significance of the "viscosity effect" in the PAV condition the unmodified binder has the consistency of light cream whereas the modified binder has the consistency of molasses. Versions of the long-term tests judged successful based on the first part of the Selection Study were subjected to this formal experiment. In this experiment, the PG 58-28 and the SBS modified PG 82-22 were aged in the prototype long-term versions of the tests and in the PAV. Rheological measurements at high, intermediate and low pavement temperatures were used to compare the level of aging to that produced by the PAV. Replication was included in this experiment to permit statistical analysis of the differences in aging that were observed. The results and analysis of this experiment are presented in detail in Section 5.

3.2 Materials

As discussed above, three binders were used in the Selection Study: a neat PG 58-28, a SBS modified PG 82-22, and an LDPE modified PG 76-22. Table 3 presents AASHTO M320 data for the binders.

Table 3. AASHTO M320 Properties for the Binders Used in the Selection Study.

Condition	Test	Method	PG 58-28	PG 82-22	PG 76-22
Unaged	Viscosity at 135 ^{o}C	ASTM D4402	0.23 Pa·s	3.19 Pa·s	2.06 Pa·s
	G*/sinδ at 10 rad/sec	AASHTO T315	1.22 kPa at 58 ^{o}C	1.94 kPa at 82 ^{o}C	1.61 kPa at 76 ^{o}C
RTFO Aged Residue	Mass Change, %	AASHTO T240	-0.358	-0.183	-0.192
	G*/sinδ, at 10 rad/sec	AASHTO T315	2.72 kPa at 58 ^{o}C	3.72 kPa at 82 ^{o}C	2.71 kPa at 76 ^{o}C
PAV Aged Residue	G*sinδ, at 10 rad/sec	AASHTO T315	2792 kPa at 19 ^{o}C	3999 kPa at 25 ^{o}C	4841 kPa at 25 ^{o}C
	Creep Stiffness, at 60 sec	AASHTO T313	218 MPa at –18 ^{o}C	177 MPa at –12 ^{o}C	218 MPa at –18 ^{o}C
	m-value at 60 sec	AASHTO T313	0.372 at –18 ^{o}C	0.335 at –12 ^{o}C	0.319 at –12 ^{o}C

The PG 58-28 and the PG 82-22 were obtained from the Paulsboro, New Jersey refinery of the Citgo Asphalt Refining Company (Citgo). The PG 82-22 binder is supplied under the trade name Citgoflex SP®. Based on information provided on the Material Safety Data Sheet for this product, Citgoflex SP® is produced with SBS polymer. The PG 76-22 binder was obtained from one of Advanced Asphalt Technologies, LLC's 2003 on-site blending projects. The PG 76-22 binder is supplied under the trade name NOVOPHALT. This particular sample contains PG 64-22 binder obtained from the Perth Amboy, New Jersey refinery of Chevron Products Co., and 6 percent LDPE.

4.0 DEVELOPMENT OF LONG-TERM AGING TESTS

4.1 Modified German Rotating Flask

Attempts to develop a prototype long-term version of the MGRF that approximates the aging produced in the PAV focused on methods to enhance mixing and to create a film that is continuously renewed within the flask. This was accomplished by adding various mixers and scrapers and varying the rotational speed of the flask. For all of this testing, a temperature of 100

°C, an air-flow rate of 36 l/hr, and an aging time of 48 hours were used. Table 4 summarizes the chronological order of the various configurations that were attempted. Figure 1 compares the degree of aging achieved with each configuration relative to the aging obtained with the PAV. Schematic diagrams of selected configurations are shown in Figures 2 through 5. The measure of the degree of aging shown in Figure 1 is defined by Equation 1. The relative aging according to this equation is simply the change in viscosity above RTFOT aging caused by the prototype long-term test divided by the increase in viscosity that occurs during PAV aging. For all equipment configurations and binders, relative aging is reported based on the dynamic viscosity measured at 60 °C and 0.1 rad/sec.

$$RA = \left(\frac{|h^*|_i - |h^*|_{RTFOT}}{|h^*|_{PAV} - |h^*|_{RTFOT}} \right) \times 100\% \qquad (1)$$

where:

RA = relative long-term aging

$|h^*|_i$ = dynamic viscosity for configuration *i*, measured at 60 °C, 0.1 rad/sec.

$|h^*|_{RTFOT}$ = dynamic viscosity for RTFOT aged, measured at 60 °C, 0.1 rad/sec.

$|h^*|_{PAV}$ = dynamic viscosity for PAV aged, measured at 60 °C, 0.1 rad/sec.

The investigation of various alternatives for a long-term version of the MGRF procedure started with the current MGRF, which uses a 2,000 ml Morton flask. The alternatives that were investigated included a 2,000 ml round flask with the addition of steel balls and rollers to enhance mixing and formation of a film and the use of scrapers to create and renew the film. As shown in Figure 1, the Morton flask was marginally successful for long-term aging for the PG 58-28, but was not successful for aging the PG 82-22. The use of a round flask with steel balls, as used in Germany, increased the aging of the PG 82-22 slightly while the use of rollers that conformed to the shape of the flask did not. The simple scrapers designed to fit in a round flask appear to remove much of the viscosity effect, resulting in similar aging of the PG 58-28 and PG 82-22 binders, but the degree of aging after 48 hours is only one-third of that obtained in the PAV.

Table 4. Summary of Long-Term Rotating Flask Configurations Tested.

Number	Flask	Mixer	Speed	Figure	Observations
1	Morton	None	4 rpm	Not shown	1. Adequate film for PG 58-22 binder. 2. Does not produce a moving film for PG 82-22 binder. 3. Low relative aging for both binders.
2	Morton	3 Steel Balls	1 rpm	Figure 2	1. Not used with PG 58-28 binder. 2. Does not produce a moving film for PG 82-22 binder. 3. Low relative aging for PG 82-22 binder
3	Round	1 Football Shaped Roller	1 rpm	Not shown	1. Not used with PG 58-28 binder. 2. Does not produce a moving film for PG 82-22 binder. 3. Low relative aging for PG 82-22
4	Round	2 Football Shaped Rollers	1 rpm	Figure 3	1. Not used with PG 58-28 binder. 2. Does not produce a moving film for PG 82-22 binder. 3. Low relative aging for PG 82-22
5	Round	Single Scraper	1 rpm	Figure 4	1. Does not produce a film for PG 58-28 binder. 2. Generated a renewed film for PG 82-22, but film thickness increased with aging time. 3. Low relative aging for both binders.
6	Round	Double Scraper	1 rpm	Figure 5	1. Not used with PG 58-28 binder 2. Generated a renewed film for PG 82-22. Film thickness relatively constant with aging time. 3. Low relative aging for PG 82-22 binders.

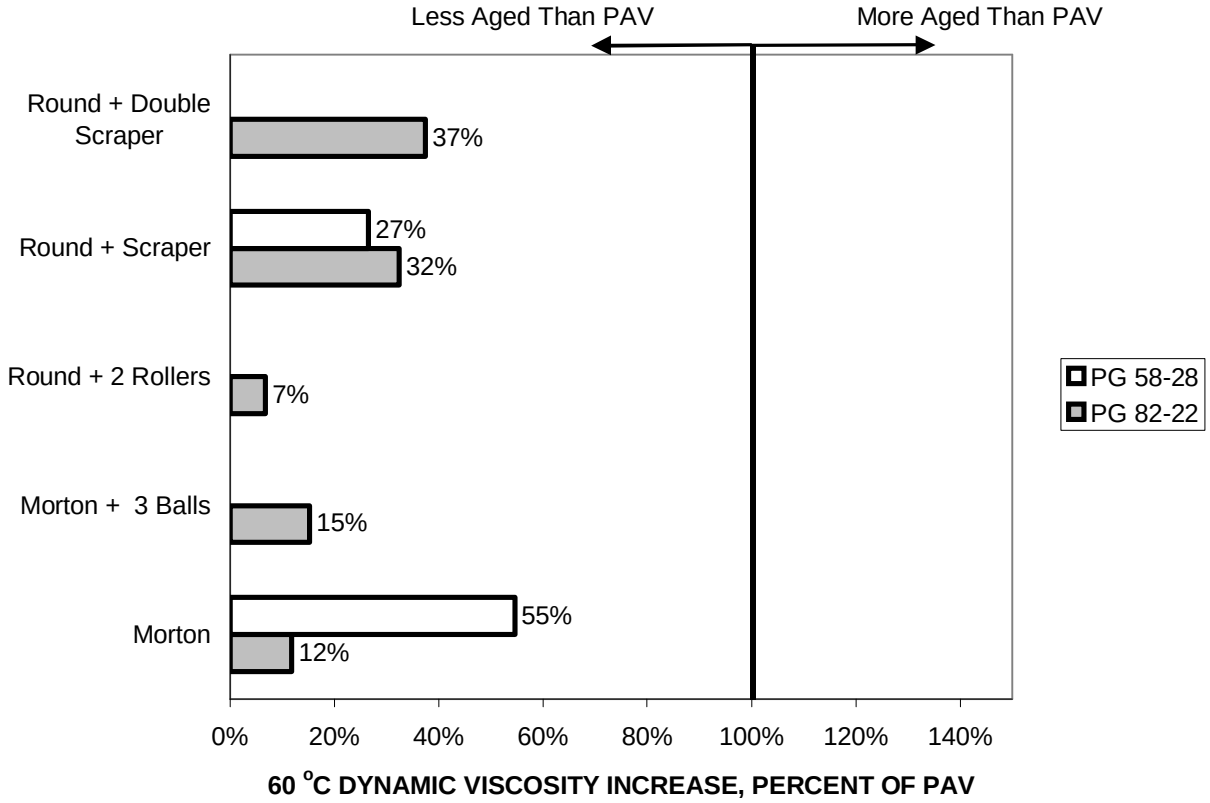

Figure 1. Relative Aging from Equation 1 for Various Long-Term Rotating Flask Configurations.

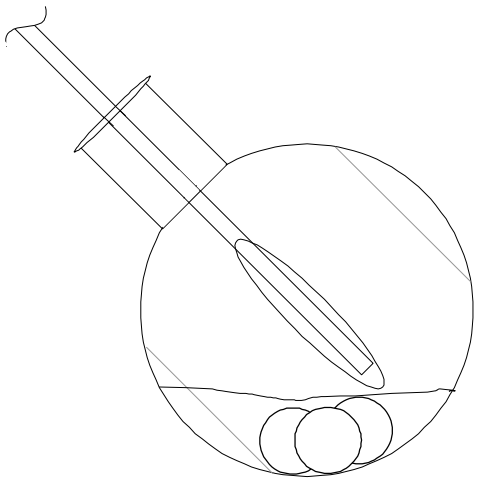

Figure 2. Schematic of 2,000 ml Morton Flask with 3 Steel Balls.

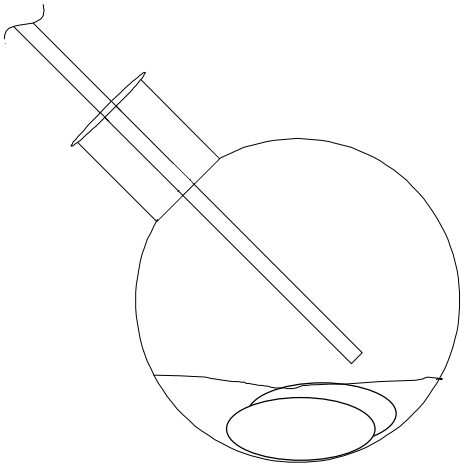

Figure 3. Schematic of 2,000 ml Round Flask With Two Football Shaped Rollers.

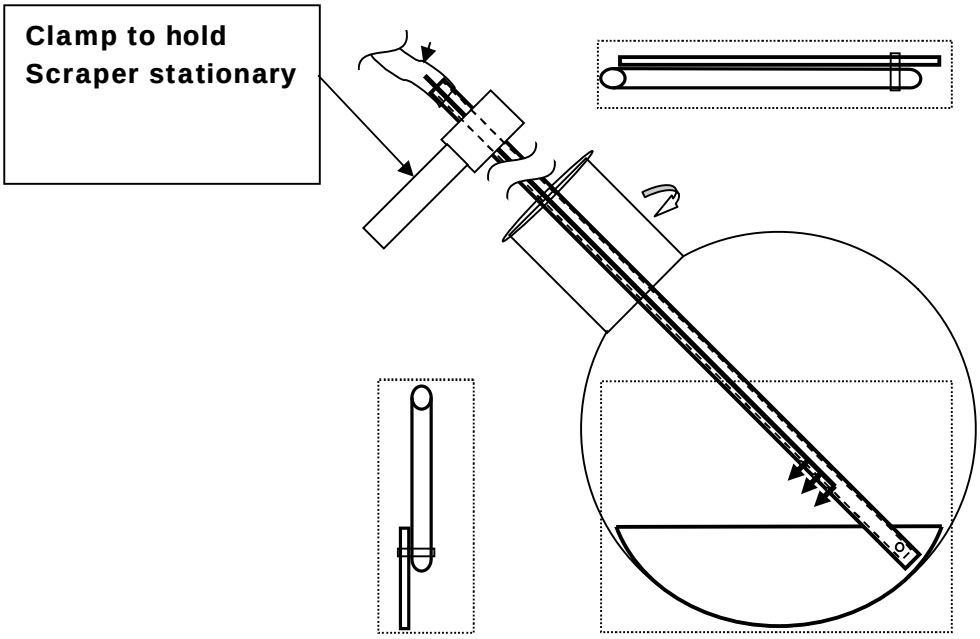

Figure 4. Schematic of 2,000 ml Round Flask With Single Scraper.

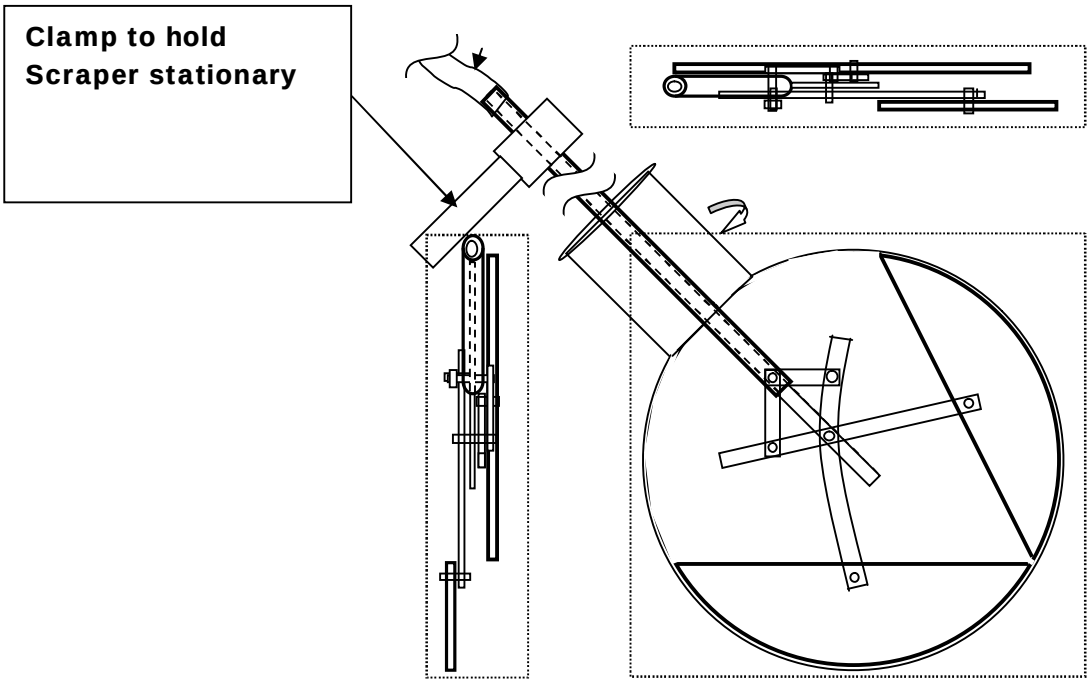

Figure 5. Schematic of 2,000 ml Round Flask With Double Scraper.

4.2 Stirred Air Flow Test

Attempts to develop a prototype long-term version of the SAFT that approximates the aging produced in the PAV focused on the design of an impeller that could efficiently mix the air with the binders over a wide range of viscosities. The design proceeded from the impeller used in the short-term version of the test, which is very efficient at mixing air with low viscosity binders, to a helix impeller which is efficient at mixing highly viscous fluids, and finally to a helix/turbine impeller which combines the benefits of both. For all of this testing, a temperature of 100 °C, and an air-flow rate of 36 l/hr were used. Table 5 summarizes the chronological order of the various configurations that were attempted. Figure 6 compares the degree of aging achieved with each configuration relative to the aging achieved with the PAV. Schematic diagrams of selected configurations are shown in Figures 7 through 9. The measure of the degree of aging shown in Figure 6 is the same used in Figure 1 and defined in Equation 1. The relative aging according to this equation is simply the change in viscosity above RTFOT aging caused by the prototype long-term test divided by the increase in viscosity that occurs during PAV aging. The dynamic viscosity was measured at 60 °C, 0.1 rad/sec.

Table 5. Summary of Long-Term Stirred Air Flow Test Configurations Tested.

Number	Impeller	Speed	Schematic	Observations
1	Original	750 rpm	Figure 7	1. Good mixing of PG 58-28 binder. 2. Could not stir PG 82-22 binder. 3. High relative aging for PG 58-28.
2	Helix	220 rpm	Figure 8	1. Good mixing of both PG 58-28 and PG 82-22 binders. 2. Better mixing of PG 82-22 binder occurs at lower speeds. 3. High relative aging of PG 82-22 binder. 4. Moderate relative aging of PG 58-28 binder.
3	Helix/ 4 bladed Turbine	350 rpm	Figure 9	1. Good mixing of PG 58-28, PG 82-22, and PG 76-22 binders. 2. Aging at 48 hrs exceeds PAV conditions for the PG 58-28 and PG 82-22. 3. Less difference in aging between PG 58-28 and PG 82-22 than observed with Helix.
4	Helix/ 8 bladed Turbine	350 rpm	Not shown	1. Good mixing of - PG 58-28, PG 82-22, and PG 76-22 binders. 2. PAV aging obtained at approximately 40 hours.

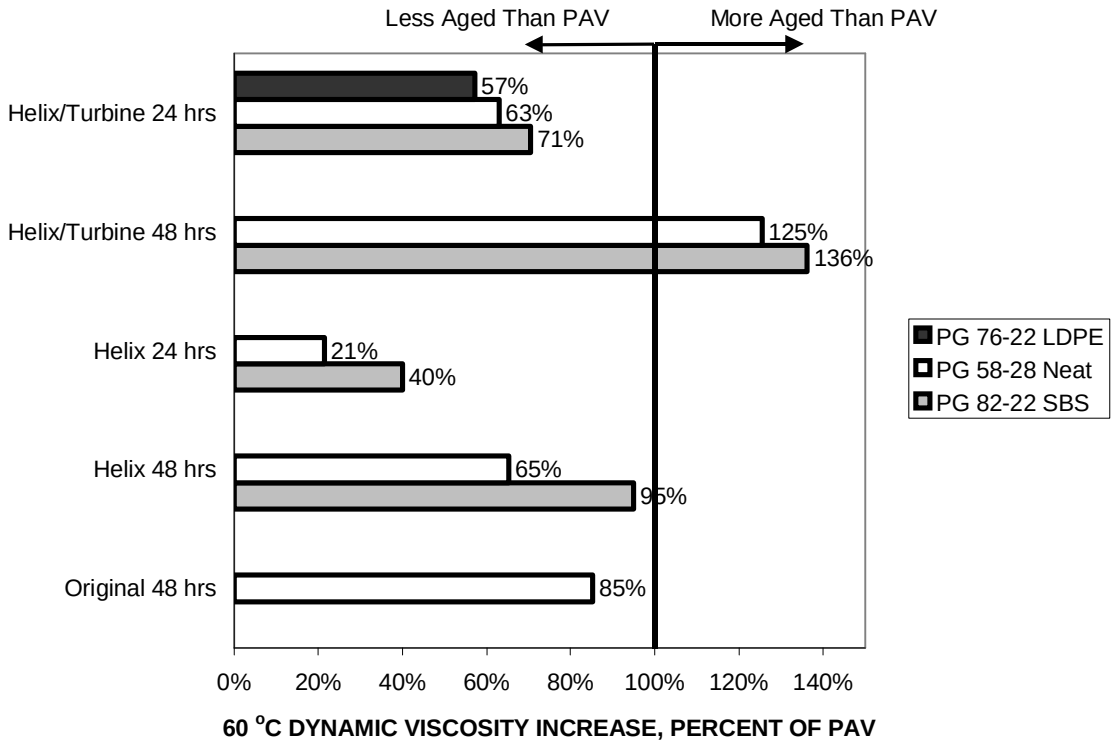

Figure 6. Relative Aging From Equation 1 for Various Long-Term Stirred Air Flow Test Configurations.

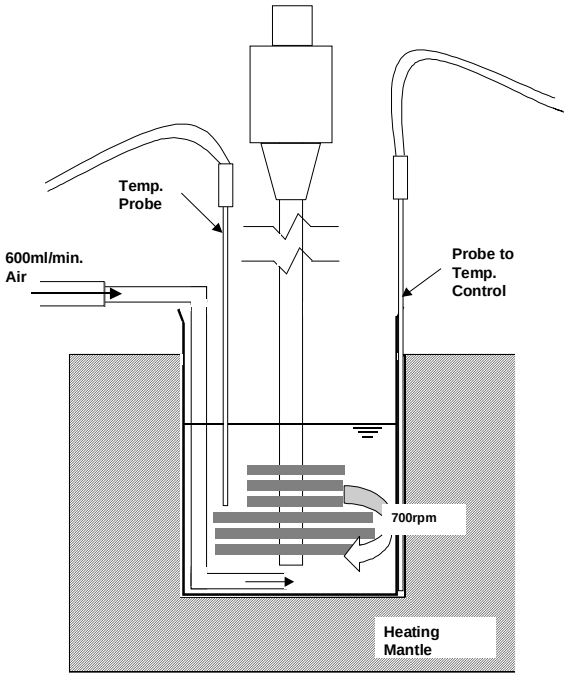

Figure 7. Schematic of Long-Term Stirred Air Flow Test With Original Impeller.

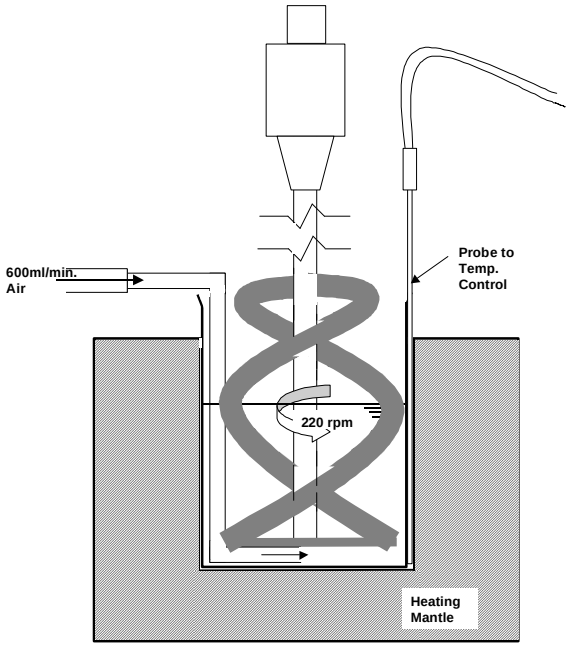

Figure 8. Schematic of Long-Term Stirred Air Flow Test With Helix Impeller.

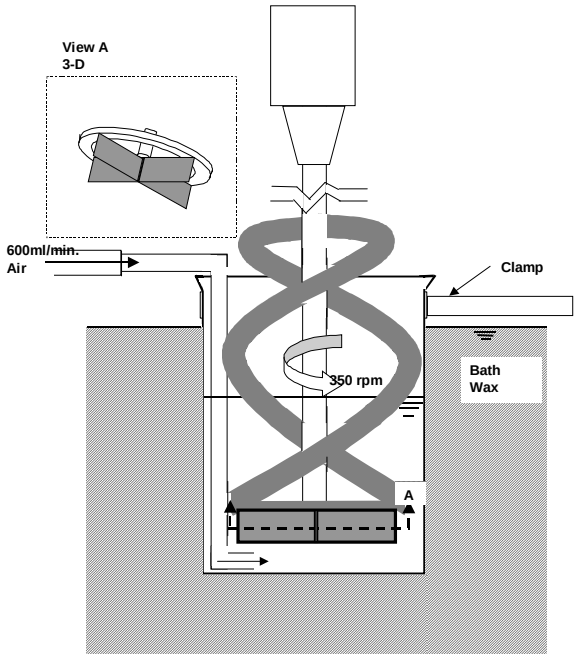

Figure 9. Schematic of Long-Term Stirred Air Flow Test With Helix/Turbine Impeller.

The original impeller worked well with the PG 58-28 binder, but it did not provide adequate mixing of the PG 82-22 binder. When this impeller is used with extremely viscous materials the entire mass of material spins with the impeller. The helix impeller, which is frequently used to

mix very viscous and particulate filled fluids, worked well with the PG 82-22 binder, but apparently did not disperse air as efficiently in the less viscous PG 58-28 binder. The helix/turbine impeller, which includes a helix to move the binder vertically in the vessel, and a turbine to mix air with the binder, resulted in the best performance over the range of binders investigated. At 48 hours, the degree of aging obtained in the PG 58-28 and the PG 82-22 binder exceeded that obtained in the PAV.

The last iteration of the impeller design was a helix/turbine impeller with 8 turbine blades. With this impeller, PAV aging conditions were reached after approximately 40 hours. Figure 10 shows the degree of aging obtained with this configuration for the three binders included in the Selection Study. The measure of the degree of aging shown in Figure 10 is the same used in Figures 1 and 6 and defined in Equation 1. The relative aging according to this equation is simply the change in viscosity above RTFOT aging caused by the prototype long-term test divided by the increase in viscosity that occurs during PAV aging. The dynamic viscosity was measured at 60 °C, 0.1 rad/sec. The degree of aging appears to increase with increasing binder stiffness which is counterintuitive.

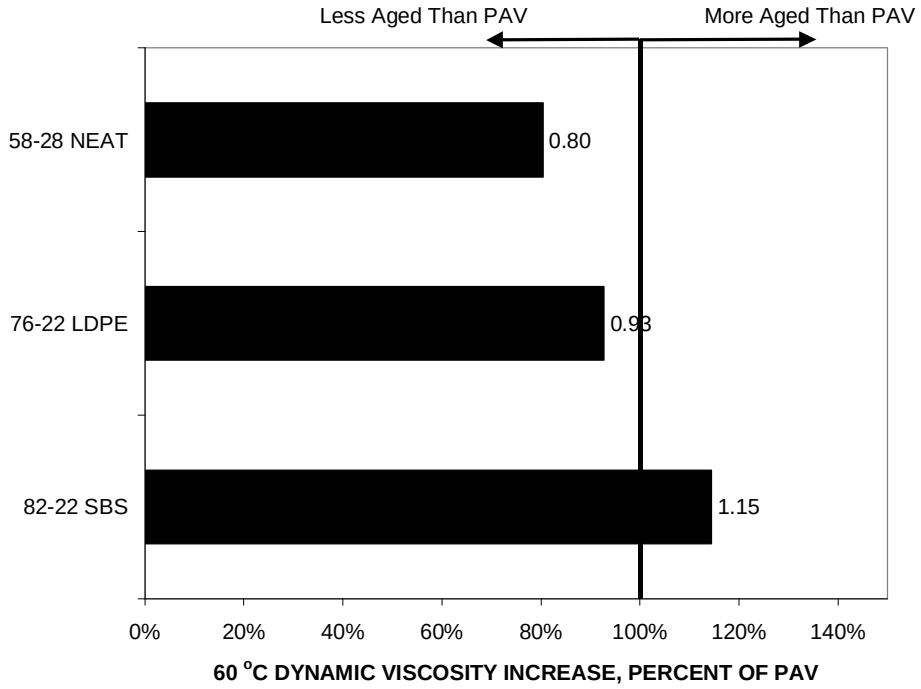

Figure 10. Relative Aging From Equation 1 for Final Iteration of the Long-Term Stirred Air Flow Test (Helix/8 Bladed Turbine, 200 rpm, 36 l/hr air-flow, 100 °C, 40 hours).

Based on the testing above, the research team concluded that it is possible to extend the SAFT to a long-term aging test. The following section discusses the viscosity effects experiment that was conducted to quantify the significance of the differences between the aging of the PG 58-28 and the PG 82-22 binder shown in Figure 10.

5.0 VISCOSITY EFFECTS EXPERIMENT

5.1 Design

Only the final iteration (a helix/turbine impeller with 8 turbine blades) of the long-term version of the SAFT was subjected to the viscosity effects experiment. Table 6 summarizes the testing conditions for the Long-Term SAFT.

Table 6. Testing Conditions for the Long-Term Stirred Air Flow Test.

Condition	Value
Sample Size	250 g
Aging Temperature	100 °C
Impeller Type	Helix + 8 Bladed Turbine
Impeller Speed	350 rpm
Air Flow Rate	36 l/hr
Aging Time	40 hours

The viscosity effects experiment was designed to investigate the effect of viscosity on the degree of aging that occurs in the Long-Term SAFT. This was accomplished by aging split samples of RTFOT-aged PG 58-28 and PG 82-22 in the PAV and the Long-Term SAFT, and comparing rheological properties at high, intermediate, and low pavement temperatures. The following properties were measured for the RTFOT, PAV, and Long-Term SAFT:

- Shear modulus and phase angle from a DSR frequency sweep at 60 °C using frequencies from 0.1 to 100 Hz.
- Shear modulus and phase angle from a DSR frequency sweep at 25 °C using frequencies from 0.1 to 100 Hz.
- Creep stiffness and m-value at 60 sec from BBR tests conducted at –12 °C.

Three independent samples were aged in the Long-Term SAFT and the PAV and tested as outlined above. The resulting data are presented in Section 8.

5.2 Statistical Analysis

Regression analysis was used to analyze the data. The data were analyzed separately for each property measured and at each test temperature as outlined below.

1. Compute averages for physical properties measured for the PAV and Long-Term SAFT residue from the three replicate samples that were aged and tested.

2. Regress the Long-Term SAFT data against the PAV data using data from both the PG 82-22 and PG 58-28 binders and a linear model with the following form:

$$P_{LTSAFT} = B_1(P_{PAV}) + B_2(P_{PAV} \text{ x } AC) \quad (2)$$

Where:

P_{LTSAFT} = measured property for Long-Term SAFT conditions (average of three replicate tests).

P_{PAV} = measured property for PAV conditions (average of three replicate tests).

AC = dummy variable for binder type (AC=0 for PG 82-22, AC=1 for PG 58-28).

B_1 and B_2 = regression coefficients

The model given in Equation 2 reduces to the following models for the PG 82-22 and the PG 58-28 binders.

For PG 82-22: $P_{LTSAFT} = B_1(P_{PAV})$ (3a)

For PG 58-28: $P_{LTSAFT} = (B_1 + B_2)(P_{PAV})$ (3b)

3. Use the regression coefficients and their standard errors from Step 2 to perform hypothesis tests on the statistical significance of the slope coefficients. With the results of the regression model check the hypothesis that the slope of the PG 82-22 data is significantly different from one, and the hypothesis that the slope of the PG 82-22 data is significantly different from that for the PG 58-28.

<u>Hypothesis Test for PG 82-22 Slope</u>

Ho: $B_1 = 1.0$, slope for 82-22 = 1.0

Ha: $B_1 \neq 1.0$, slope for 82-22 $\neq$ 1.0

Test Statistic: $t = \frac{B_1 - 1.0}{S_e(B_1)}$

Where:

$S_e(B_1)$ = standard error of B_1

Region of Rejection: Reject H_o if $t < -t_{\alpha/2}$ or $t > t_{\alpha/2}$ for n-2 degrees of freedom.

Hypothesis Test for Difference Between PG 82-22 and PG 58-28 Slopes

Ho: $B_2 = 0$, slope for 82-22 and PG 58-28 are the same

Ha: $B_2 \neq 0$, slope for 82-22 ≠ slope for PG 58-28

Test Statistic: $t = \frac{B_0 - 0.0}{S_e(B_2)}$

Where:

$S_e(B_2)$ = standard error of B_2

Region of Rejection: Reject H_o if $t < -t_{\alpha/2}$ or $t > t_{\alpha/2}$ for n-2 degrees of freedom.

4. Regress the Long-Term SAFT data against the PAV data using only the data from the PG 58-28 binder and a linear model with the following form:

$$P_{LTSAFT} = B_3(P_{PAV}) \quad (4)$$

5. Use the regression coefficient and its standard error from Step 4 to perform a hypothesis test on the statistical significance of the slope coefficient. With this model check if the slope for the PG 58-28 data is significantly different than one.

Hypothesis Test for PG 82-22 Slope

Ho: $B_3 = 1.0$, slope for 58-28 = 1.0

Ha: $B_1 \neq 1.0$, slope for 58-28 ≠ 1.0

Test Statistic: $t = \frac{B_3 - 1.0}{S_e(B_3)}$

Where:

$S_e(B_3)$ = standard error of B_3

Region of Rejection: Reject H_o if $t < -t_{\alpha/2}$ or $t > t_{\alpha/2}$ for n-2 degrees of freedom.

The sections that follow present and discuss the findings of these analyses for the three temperature conditions.

High Pavement Temperature Properties

Properties measured at the high pavement temperature included shear modulus and phase angle for a frequency sweep conducted at 60 °C using frequencies from 0.1 to 100 Hz. Figures 11, 12, and 13 compare the shear modulus and phase angle data collected at 60 °C. Figures 11 and 12 present the shear modulus data. The scale is expanded in Figure 12 to better show the low modulus data. The phase angle data are presented in Figure 13. In all of these figures averages from three replicate tests on the residue from the Long-Term SAFT and the PAV are shown.

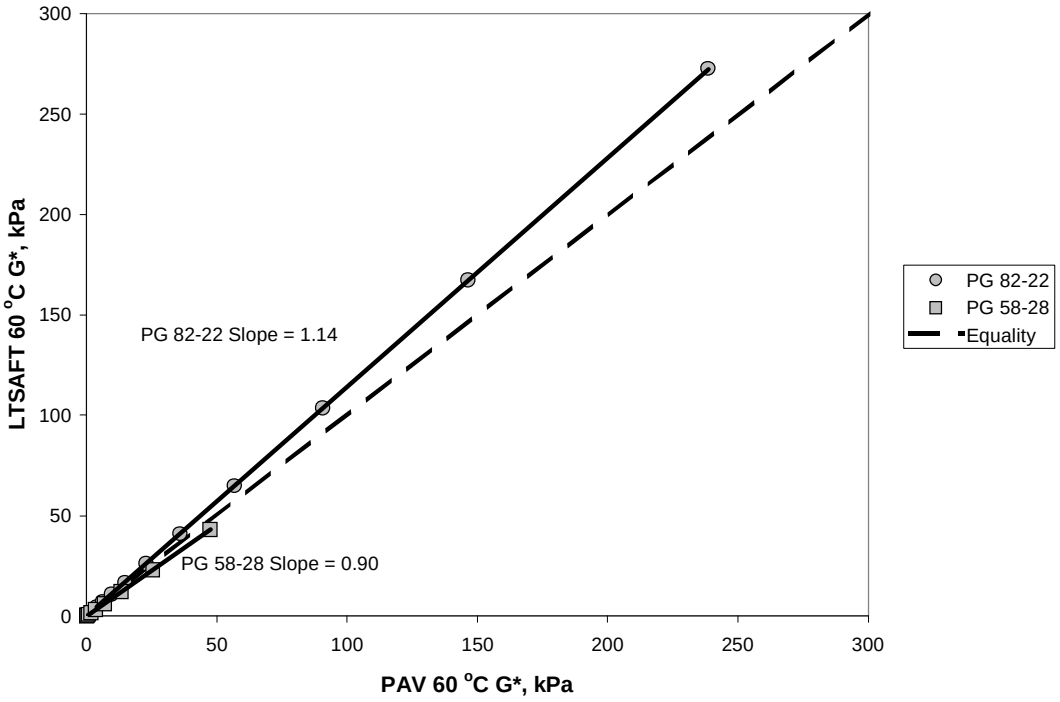

Figure 11. 60 °C Shear Modulus Data, Full Range.

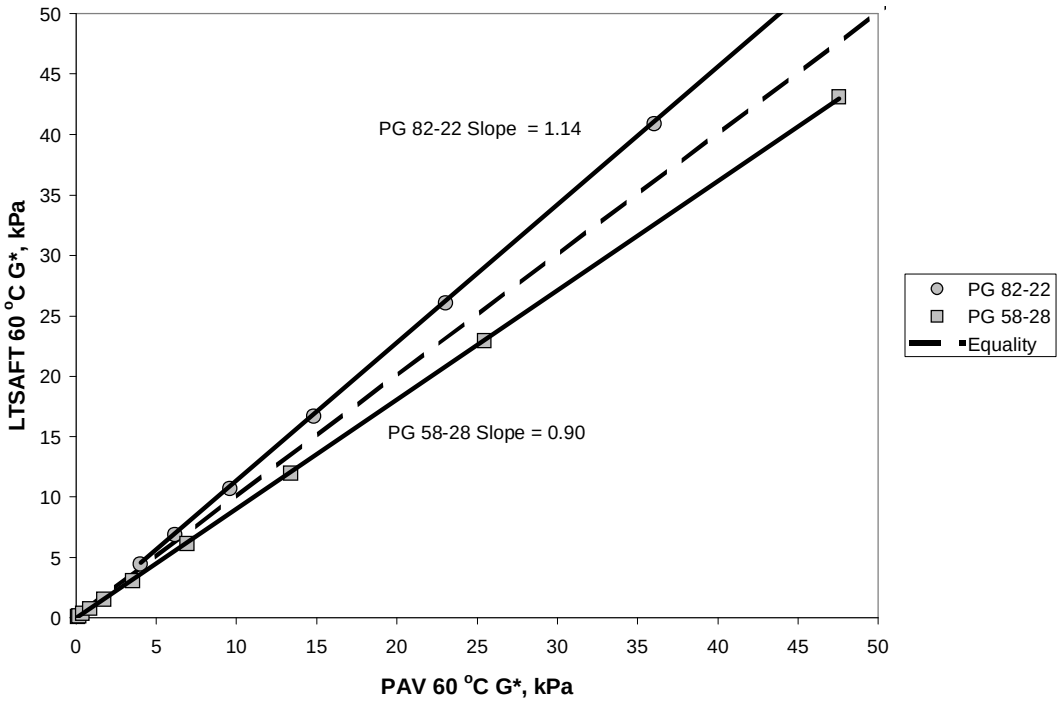

Figure 12. 60 °C Shear Modulus Data, Expanded Scale.

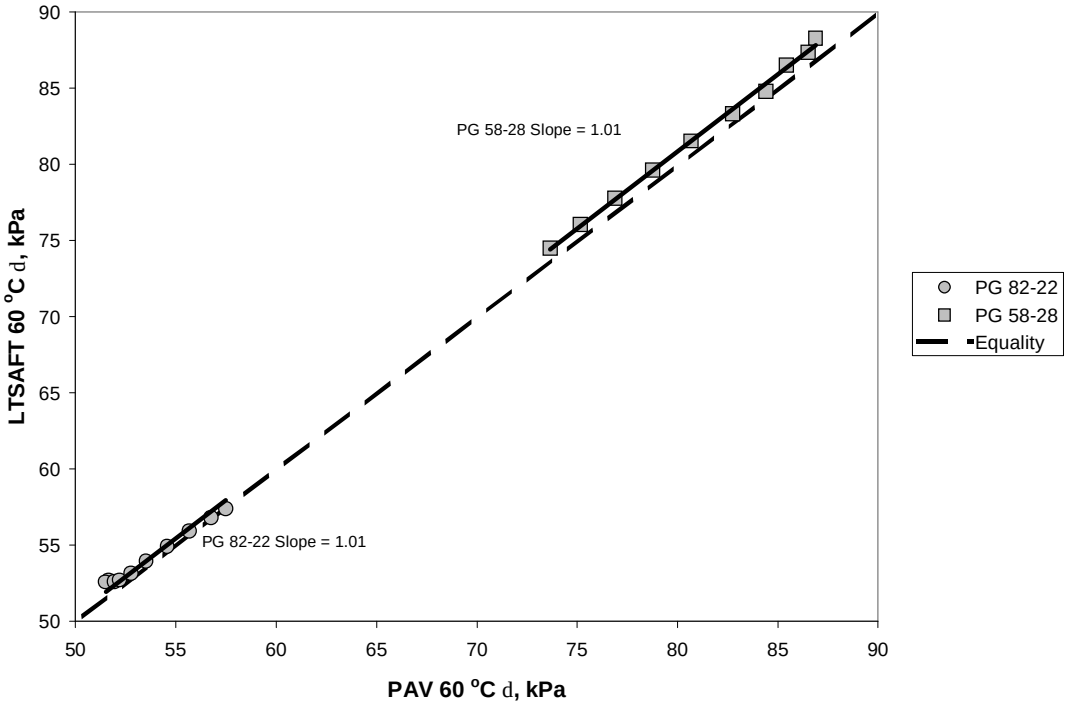

Figure 13. 60 °C Phase Angle Data.

The statistical analysis of these data is summarized in Table 7. This analysis produced the following findings for the DSR data obtained at the high pavement temperature:

1. The shear modulus of the PG 82-22 binder is significantly higher when aged in the Long-Term SAFT compared to PAV aging. The magnitude of the bias is 14 percent.
2. The shear modulus of the PG 58-28 binder is significantly lower when aged in the Long-Term SAFT compared to PAV aging. The magnitude of the bias is 10 percent.
3. The relative aging measured by the shear modulus at 60 °C shows a significant binder effect. The Long-Term SAFT ages the PG 58-28 binder less than the PAV, while it ages the PG 82-22 binder more than the PAV.
4. The phase angle for both binders is significantly higher when aged in the Long-Term SAFT compared to PAV aging. The magnitude of the bias is 1 percent. Although this bias is statistically significant, from an engineering standpoint the phase angles are essentially equivalent.

Table 7. Summary of Statistical Analysis of High Pavement Temperature DSR Data.

Property	Coefficient	Value	Se	t	dof	$t_{cr,\ a = 0.05}$	Conclusion
G*	B_1	1.1411	0.00050	284.271	18	2.101	PG 82-22 Slope > 1.0
	B_2	-0.2369	0.00273	-86.880	18	-2.101	PG 58-28 Slope < PG 82-22 Slope
	B_3	0.9042	0.00160	-60.024	8	-2.306	PG 58-28 Slope < 1.0
δ	B_1	1.0094	0.0022	4.338	18	2.101	PG 82-22 Slope > 1.0
	B_2	0.0003	0.0025	0.124	18	2.102	PG 58-28 Slope = PG 82-22 Slope
	B_3	1.0103	0.0010	10.210	8	2.306	PG 58-28 Slope > 1.0

Intermediate Pavement Temperature Properties

Properties measured at the intermediate pavement temperature included of shear modulus and phase angle for a frequency sweep conducted at 25 °C using frequencies from 0.1 to 100 Hz. Figures 14, 15, and 16 compare the shear modulus and phase angle data collected at 25 °C. Figures 14 and 15 present the shear modulus data. The scale is expanded in Figure 15 to better show the low modulus data. The phase angle data are presented in Figure 16. In all of these figures averages from three replicate tests of the residue of the Long-Term SAFT and the PAV are shown.

The statistical analysis of these data is summarized in Table 8. This analysis produced the following findings for the intermediate pavement temperature DSR data:

1. The shear modulus of the PG 82-22 binder is significantly higher when aged in the Long-Term SAFT compared to PAV aging. The magnitude of the bias is 13 percent.
2. The shear modulus of the PG 58-28 binder is significantly lower when aged in the Long-Term SAFT compared to PAV aging. The magnitude of the bias is 6 percent.
3. The relative aging measured by the shear modulus at 25 °C shows a significant binder effect. The Long-Term SAFT ages the PG 58-28 binder less than the PAV, while it ages the PG 82-22 binder more that the PAV.
4. The phase angle for the PG 82-22 binder is significantly lower when aged in the Long-Term SAFT compared to PAV aging. The magnitude of the bias is 2 percent; statistically significant but perhaps not significant from an engineering standpoint.
5. The phase angle for the PG 58-28 binder is significantly higher when aged in the Long-Term SAFT compared to PAV aging. The magnitude of the bias is 1 percent; again statistically significant but perhaps not significant from an engineering standpoint.
6. The relative aging measured by the phase angle at 25 °C shows a significant binder effect. The Long-Term SAFT ages the PG 58-28 binder less than the PAV, while it ages the PG 82-22 binder more that the PAV.

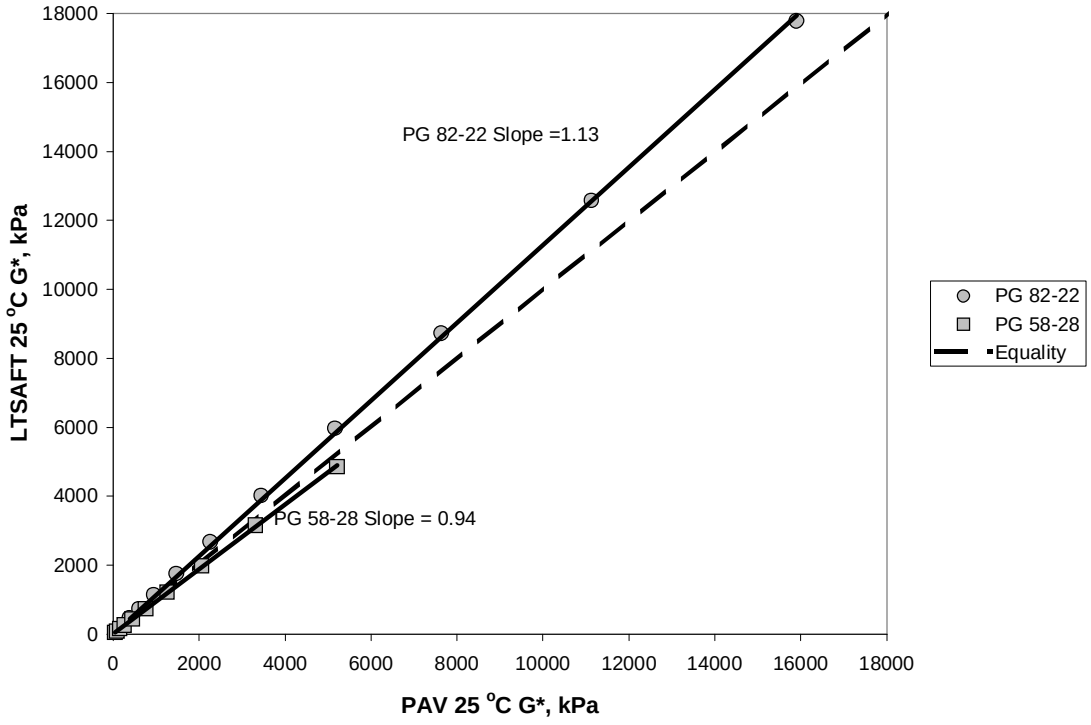

Figure 14. 25 °C Shear Modulus Data, Full Range.

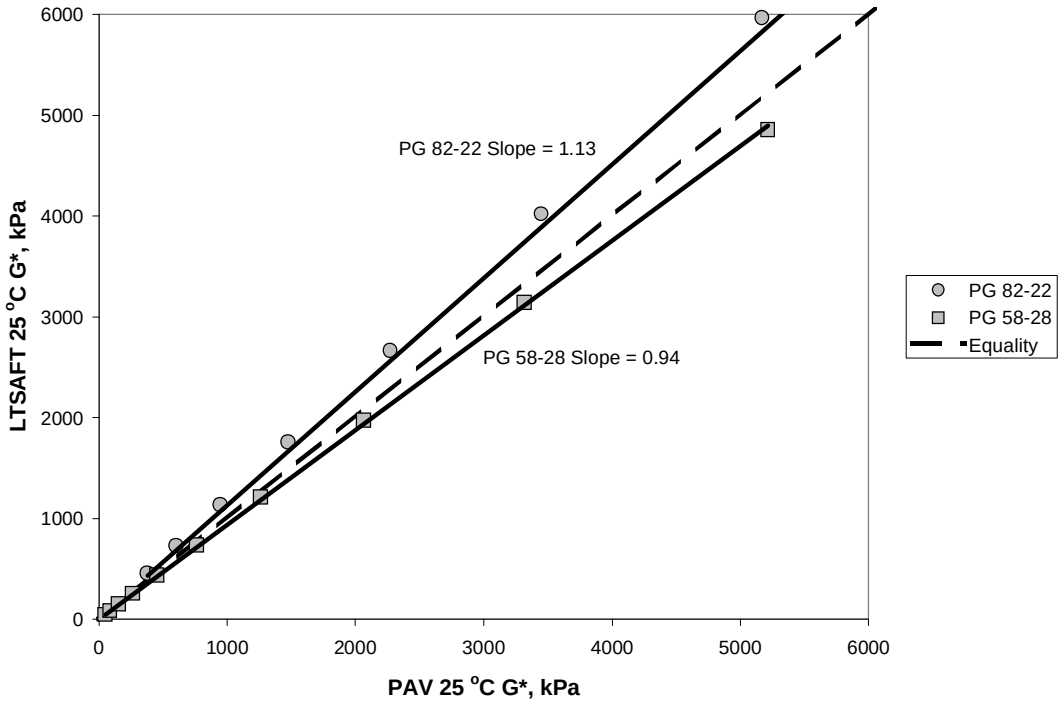

Figure 15. 25 °C Shear Modulus Data, Expanded Scale.

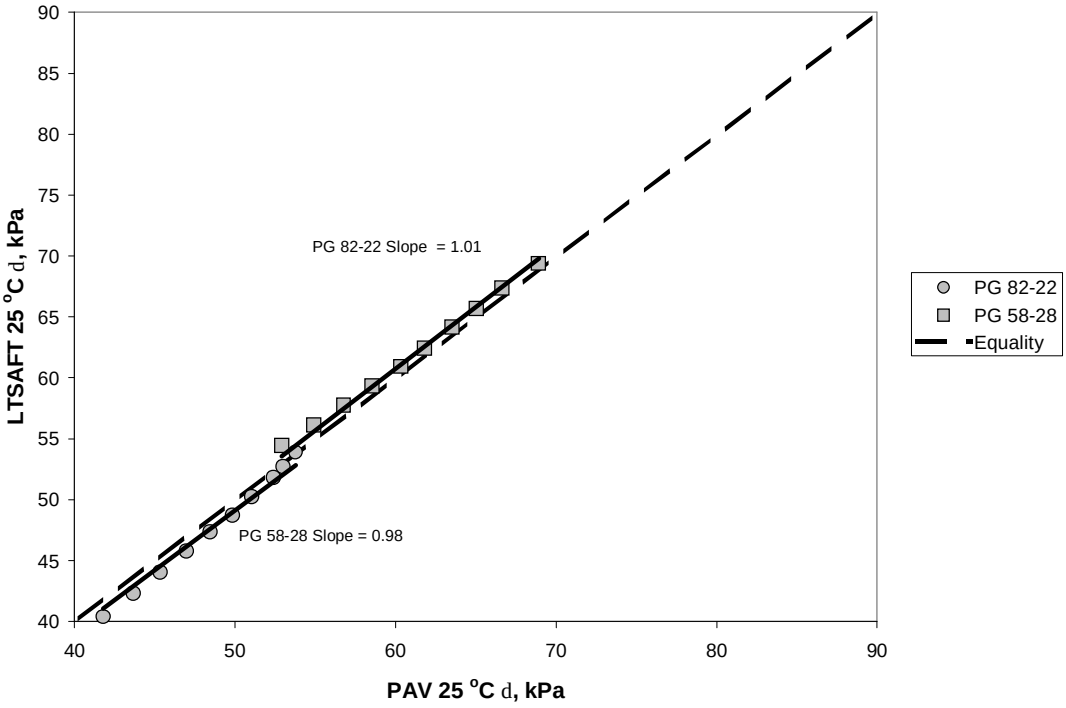

Figure 16. 25 °C Phase Angle Data.

Table 8. Summary of Statistical Analysis of Intermediate Pavement Temperature DSR Data.

Property	Coefficient	Value	Se	t	dof	$t_{cr,}$ a = 0.05	Conclusion
G*	B_1	1.1271	0.0035	36.366	18	2.101	PG 82-22 Slope > 1.0
	B_2	-0.1884	0.0120	-15.728	18	-2.101	PG 58-28 Slope < PG 82-22 Slope
	B_3	0.9387	0.0035	17.384	8	2.306	PG 58-28 Slope < 1.0
δ	B_1	0.9819	0.0032	-5.692	18	-2.101	PG 82-22 Slope < 1.0
	B_2	0.0308	0.0041	7.573	18	2.101	PG 58-28 Slope > PG 82-22 Slope
	B_3	1.0127	0.0020	6.443	8	2.306	PG 58-28 Slope > 1.0

Low Temperature Properties

The low pavement temperature properties included measurements of the creep modulus and m-value at -12 °C. Data were collected at the six standard times (8, 15, 30, 60, 120, and 240 sec) reported in the BBR test. Figures 17 and 18 compare the creep modulus and m-value data. In both figures averages from six replicate beams prepared from material aged in the Long-Term SAFT and the PAV are shown.

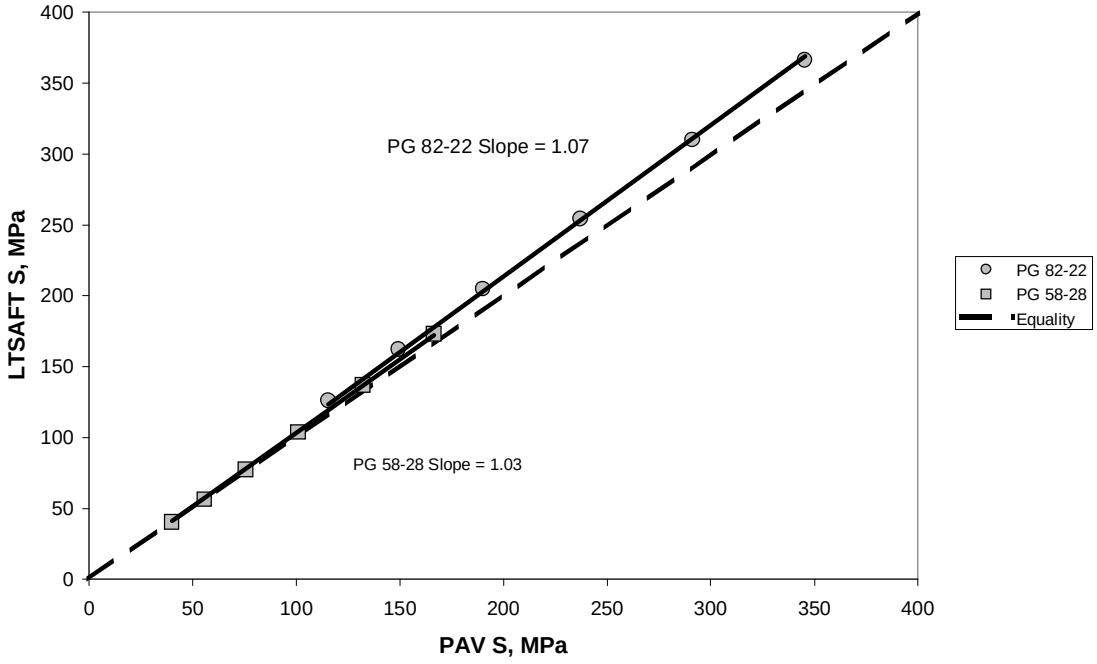

Figure 17. -12 °C Creep Modulus Data.

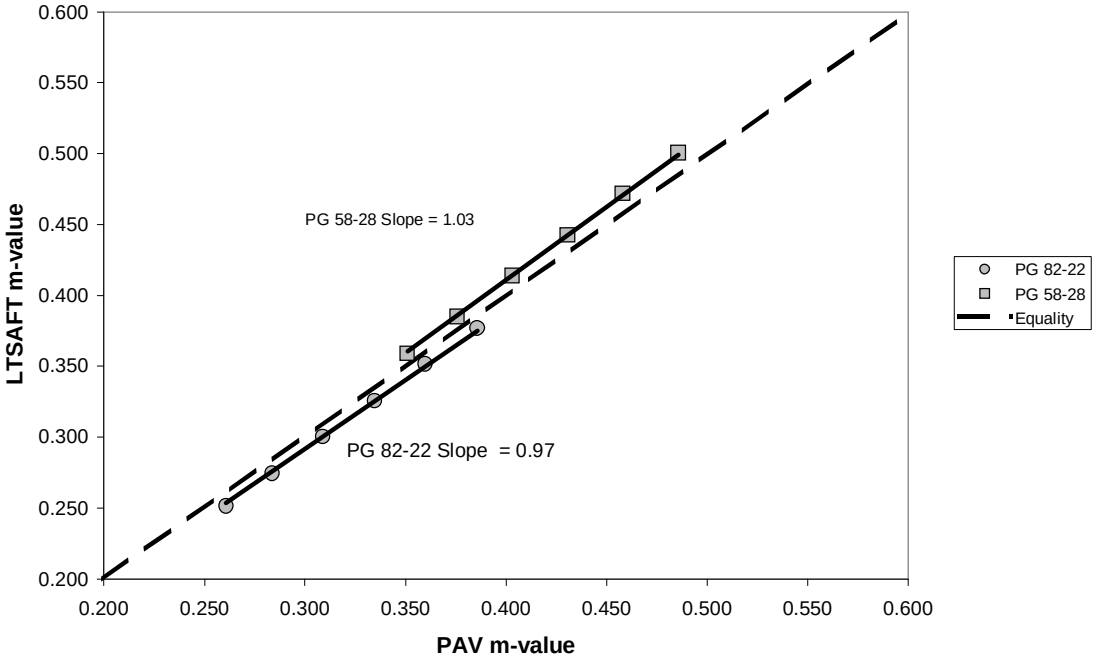

Figure 18. –12 °C m-Value Data.

The statistical analysis of these data is summarized in Table 9. This analysis produced the following findings the low pavement temperature BBR data:

1. The creep modulus of the PG 82-22 binder is significantly higher when aged in the Long-Term SAFT compared to PAV aging. The magnitude of the bias is 7 percent.
2. The creep modulus of the PG 58-28 binder is also significantly higher when aged in the Long-Term SAFT compared to PAV aging. The magnitude of the bias is 3 percent.
3. The relative aging measured by the creep modulus at –12 °C shows a significant binder effect. Although the Long-Term SAFT ages both binders more than the PAV, the bias is less for the PG 58-28 binder compared to the PG 82-22 binder.
4. The m-value for the PG 82-22 binder is significantly lower when aged in the Long-Term SAFT compared to PAV aging. The magnitude of the bias is 3 percent.
5. The m-value for the PG 58-28 binder is significantly higher when aged in the Long-Term SAFT compared to PAV aging. The magnitude of the bias is 3 percent.
6. The relative aging measured by the m-value at -12 °C shows a significant binder effect. The Long-Term SAFT ages the PG 58-28 binder less than the PAV, while it ages the PG 82-22 binder more than the PAV.

Table 9. Summary of Statistical Analysis of Low Pavement Temperature DSR Data.

Property	Coefficient	Value	Se	t	dof	$t_{cr,}$ a = 0.05	Conclusion
S	B_1	1.0683	0.0031	21.737	10	2.228	PG 82-22 Slope > 1.0
	B_2	-0.0366	0.0077	-4.737	10	-2.228	PG 58-28 Slope < PG 82-22 Slope
	B_3	1.0317	0.0042	7.500	4	2.776	PG 58-28 Slope > 1.0
m	B_1	0.9728	0.0019	-14.509	10	-2.101	PG 82-22 Slope < 1.0
	B_2	0.0550	0.0024	23.215	10	2.101	PG 58-28 Slope > PG 82-22 Slope
	B_3	1.0278	0.0012	23.475	4	2.776	PG 58-28 Slope > 1.0

5.3 Engineering Analysis

The statistical analysis of the viscosity effects experiment showed a difference in the degree of aging for samples aged in the Long-Term SAFT and the PAV. For stiffness measurements, the bias ranged from as high as 14 percent for high pavement temperature shear modulus measurements to as low as 3 percent for low temperature creep modulus measurements. Bias in

the phase angle and m-value were generally smaller ranging from 1 to 3 percent. The regression approach used in the analysis of the data is very effective at identifying bias between two measurements. The phase angle bias was only 1 percent, and from an engineering perspective has little effect on the AASHTO T320 specification measurements. The shear modulus, creep stiffness, and m-value biases were larger. Table 10 compares these biases with single operator precision statements as published in AASHTO T313 (BBR) and AASHTO T315 (DSR). The biases are approximately two times the coefficient of variation for single operator tests.

Table 10. Comparison of Long-Term Stirred Air Flow Test Bias With DSR and BBR Precision.

Property	Long-Term Stirred Air Flow Test Bias	AASHTO Single Operator Coefficient of Variation
G* at 60 °C	-10 to +14 %	7.9 %
G* at 25 °C	-6 to +13 %	7.9 %
S	+3 to +7 %	3.2 %
m	-3 to +3 %	1.4 %

Probably more important than the finding that the aging is different between the two tests is the fact that the two binders aged differently. The PG 82-22 binder aged more in the Long-Term SAFT than in the PAV, while the PG 58-28 binder aged more in the PAV than in the Long-Term SAFT. This difference is most evident in the high pavement temperature tests, but also occurs in the intermediate and low pavement temperature tests that are used in AASHTO M320. Differences between the aging produced by the Long-Term SAFT and the PAV appear to be temperature dependent. The differences are greater at the upper grading temperature than at the lower grading temperature. This implies that the two aging procedures produce materials that are different rheologically.

There are two possible explanations for the binder effect. First, the helix/turbine impeller and its rotational speed may not be properly optimized for lower viscosity binders. Second, the air dispersion mechanism in the Long-Term SAFT test may age polymers more than or in a different way than the high-pressure aging occurring in the PAV. Additional testing of neat and modified

binders, both having a wide range of consistency is needed to determine the cause of this effect and to further improve the Long-Term SAFT.

6.0 SUMMARY AND CONCLUSIONS

During Phase I of Project 9-36 it was concluded that both the MGRF and the SAFT are promising approaches for an improved short-term aging procedure that can be used in the United States in conjunction with AASHTO M320. Both tests require relatively inexpensive equipment, are easy to perform, and are applicable to both neat and modified binders. Most importantly, they reasonably reproduce the level of aging that occurs in the RTFOT. The major issue left unresolved by the Phase I literature review and review of research in progress was which of these two tests is best suited to further development as a long-term aging test. Since cost, complexity, applicability to neat and modified binders, and the ability to simulate the RTFOT were all judged to be similar for the two tests, the extendibility to long-term aging became an important factor in selecting the test method that will be further developed in Project 9-36.

The Selection Study documented in this report was designed to investigate the extension of these two tests to long-term aging. It was designed to examine the degree of long-term aging that can be obtained in both tests using practical test conditions and to determine if the degree of aging is significantly affected by the viscosity of the binder. Based on the testing and analysis presented in this report, the following conclusions were drawn:

1. **MGRF.** It does not appear that further effort to extend the MGRF to long-term aging is warranted. This method is designed to expose a thin film of binder to air or oxygen. The amount of aging that occurs depends upon the thickness of the film and the thickness of the film is dependent upon the degree of mixing that occurs during test. Unfortunately both of these effects depend upon the viscosity of the binder. These effects are exacerbated at the lower, long-term aging temperature where the viscosity of all binders is much greater than at the short-term aging temperature. Consequently, mechanical mixing is required to minimize the viscosity effect. Adding steel balls or rollers is only marginally beneficial. There is a possibility that a mechanical wiper may provide a more uniform film, but the viscosity of the binder is still likely to affect the effectiveness of the wiper.

This approach was found to be impractical with glass flasks because glass blowing tolerances make it difficult to control the film thickness of the binder. Without some sort of mechanical wiper and machined vessel, further effort to apply the thin film approach does not appear warranted for long-termed aging. The Rolling Cylinder Aging Test uses a heavy roller inside a cylindrical vessel to produce an approximately 2-mm thick film. This test requires approximately 144 hours to produce levels of aging comparable to those obtained in the PAV.

2. **SAFT.** It appears that with additional development, the SAFT can be modified for use as a long-term aging test. This method is designed to bubble air through a mass of the binder, thereby exposing the binder to oxygen. As with the MGRF, adequate mixing of the binder is important and this is obtained through selection of a proper impeller. Additionally, the impeller must adequately break-up or disperse the air to accelerate the long-term aging process. During the Selection Study, a helix/turbine impeller was developed for the Long-Term SAFT. With this impeller, aging comparable to that occurring in the PAV can be obtained for a wide range of binders. Two modifications of the SAFT are needed to extend it to long-term aging. First, different impellers are needed for the short- and long-term tests. Second, the stirring motor used in the short-term test was inadequate and the size of the motor must be increased substantially to accommodate the high torque required to turn the helix/turbine impeller in highly viscous materials.

   The duration of the procedure is somewhat long at 40 hours, and there is a binder effect. For the same operating conditions, stiffer polymer modified binders tend to age more relative to PAV aging than softer neat binders. It is likely that the duration of the test can be further reduced through refinement of the impeller, use of enriched air, and optimization of other operating parameters such as rotational speed and air flow rate. Additional study is needed to determine the source of the binder effect and to further modify the procedure to overcome this effect.

7.0 RECOMMENDATIONS

7.1 Phase II of Project 9-36

Based on the findings of the Phase I and the Selection Study, the research team recommends that the SAFT be further developed as an improved short-term aging procedure in Phase II of Project 9-36. The Phase I literature review and review of research in progress concluded the Stirred Air Flow Test is relatively inexpensive, easy to perform, applicable to both neat and modified binders, and reasonably reproduces the level of aging that occurs in the RTFOT. The Selection Study reported in this document concluded that with additional developmental effort, the SAFT can likely be extended to long-term aging. Two scenarios for using the SAFT in AASHTO M320 are discussed below.

Stirred Air Flow Test as a Replacement for the RTFOT

The first scenario is to replace the RTFOT with the SAFT as the short-term aging procedure and to continue to use the PAV for long-term aging. Table 11 compares the SAFT test and the RTFOT for short-term aging.

Table 11. Comparison of Stirred Air Flow Test and RTFOT.

Considerations	Rolling Thin Film Oven	Stirred Air Flow Test
Neat and Modified Binders	No	Yes
Amount of Material	280 g (8 bottles)	250 g
Equipment Cost	$7,500	$6,500
Equipment Complexity	Moderately Complex	Moderately Complex
Current Availability	High	Low
Test Complexity	Reasonable	Reasonable
Binder Recovery	Difficult	Easy
Clean-up	Ignition Oven	Solvent
Temperature	163 °C	163 °C
Duration	85 min	45 min
Atmosphere	Air at 4 L/min	Air at 2 L/min
Measure Volatility	Mass Change	Volatile recovery system

The advantages of the SAFT for short-term aging are:

- Applicable to both neat and modified binders.
- Shorter test duration.
- Easier recovery of aged binder.
- Includes a volatile compound recovery system.
- Slightly lower equipment cost.

Of these, its applicability to both neat and modified binders and the potential for developing an effective volatile recovery system are the most significant advantages. The well documented problems associated with aging modified binders in the RTFOT were part of the justification for Project 9-36. Research completed during the development of the SAFT at Texas A&M University and work completed in Project 9-36 during the Selection Study shows that the test can be used to age stiff, modified binders. With further refinement, the volatile compound recovery system included in the SAFT represents an improvement over the mass change approach used in the RTFOT.

The disadvantages of the SAFT for short-term aging are:

- There is currently only a single manufacturer of the equipment although this disadvantage will likely be overcome if the procedure is adopted for specification use.
- Solvent clean-up is needed for components with bearings and mating machined surfaces.
- Only a single binder can be aged during an equipment cycle.

This last disadvantage is probably the most serious. With the RTFOT, more than one binder can be aged during each cycle in the aging oven . Although this of no significance when complete AASHTO M320 or AASHTO MP1a grading is being performed, it is a consideration when a quality control or acceptance program combines frequent DSR tests on short-term aged material with a limited number of DSR and BBR tests on long-term aged material. For such a program,

the shorter duration of the SAFT is offset by the fact that multiple binders that can be aged simultaneously in the RTFOT.

In summary, for complete AASHTO M320 and AASHTO MP1a grading, replacing the RTFOT with the SAFT offers several advantages for short-term aging. The most important are the SAFT can be used with both modified and unmodified binders and, with further development, has the potential for providing a direct measurement of the volatile loss that occurs during the aging process. The test also offers some operational advantages including a shorter test duration, easier recovery of the aged binder, and a slightly lower equipment costs.

Stirred Air Flow Test as a Replacement for the RTFOT and the PAV

The second scenario is to use the SAFT for both short and long-term aging. Based on the limited testing performed during the Selection Study, it is possible to approximate PAV conditions using the SAFT. Two modifications of the current device are needed to extend it to long-term aging. First, different impellers are needed for the short- and long-term tests. Second, the size of the motor must be increased substantially to accommodate the high torque required to turn the impeller for the long-term test in highly viscous materials. Table 12 compares the prototype version of the Long-Term SAFT and the PAV for long-term aging.

As shown in Table 12, there are two fundamental advantages that Long-Term SAFT has over the PAV. First, the binder is aged at atmospheric pressure eliminating the safety concerns that have been expressed for the PAV. Second, multiple sampling times can be included in the procedure to assess aging kinetics. The basic device is also less expensive than the current PAV. The major disadvantage of the SAFT for long-term aging is the test will likely require longer than the 20 hour cycle time for the PAV and only a single binder can be aged during the test. However, the cycle time should be less than 48 hours making it a two-day instead of a one-day test.

Table 12. Comparison of Stirred Long-Term Stirred Air Flow Test and PAV.

Considerations	PAV	Long-Term Stirred Air Flow Test
Neat and Modified Binders	Yes	Yes
Amount of Material	500 g (10 pans)	250 g
Number of Binders per Equipment Cycle	2	1
Equipment Cost	$12,500	$6,500
Equipment Complexity	Simple	Moderately Complex
Availability	High	Low
Test Complexity	Reasonable	Reasonable
Safety Precautions	High Air Pressure	None
Binder Recovery	Easy	Easy
Clean-up	Solvent	Solvent
Sampling During Test	No	Yes
Temperature	90, 100, 110 °C	*³ 100 °C **
Duration	20 hours	*Approx. 40 hours **
Atmosphere	Air pressurized to 2.1 MPa	*Air flowing at 36 L/hr **

** Conditions in italics are estimated based on limited testing.*

7.2 Additional Future Research

The expected products of Phase II of Project 9-36 will be an improved short-term binder aging procedure based on the SAFT that produces the same degree of aging as the RTFOT for neat binders, and a verification of the procedure for neat and modified binders using data from oven-aged mixtures. Additional research beyond Phase II of Project 9-36 will clearly be needed to adequately address long-term aging. While Project 9-36 is charged with developing a work plan to extend the SAFT to long-term aging, other issues associated with long-term aging should also be considered by the NCHRP. Based on work completed during the Selection Study, it appears that long-term aging in the SAFT will likely take significantly longer (approximately 40 hours) than the PAV aging time of 20 hours. Therefore, the PAV may remain the long-term aging test of choice for specification testing. Future research into long-term aging should include work with the PAV in addition to the Long-Term SAFT and other alternatives that may be identified in the future. This work should generally be directed at establishing operating conditions for simulated laboratory aging tests that reproduce the degree of aging that occurs in field pavements for typical binders. Mirza and Witczak's Global aging model, while highly

empirical, provides an estimate of site specific aging based on an analysis of historical data. Work in Project 9-23 that was reviewed during Phase I shows that the PAV operated at 100 °C for 20 hours under 2.1 MPa air pressure produces aged binders with viscosities that are in reasonable agreement with this model for a time of 10 years and moderate mean annual air temperature conditions. Based on this finding the potential for the development of a long-term aging procedure that represents a reasonable period of service in the field is encouraging.

8.0 VISCOSITY EFFECTS EXPERIMENT TEST DATA

Table 13. DSR Frequency Sweep Data for the PG 58-28 Binder.

		Temp, C	Property	Freq.(rad/s)									
Replicate	Condition			0.10	0.22	0.46	1.00	2.15	4.64	10.00	21.54	46.41	100.00
1	RTFOT	60	G*, Pa	23	48	105	225	477	1002	2073	4227	8505	16730
			d	89.6	88.6	89.2	88.3	87.3	86.1	84.7	83.4	82.0	80.7
		25	G*, Pa	10160	19760	37520	70580	130300	238400	430700	768200	1345000	2300000
			d	78.3	76.4	74.5	73.1	71.6	70.1	68.7	67.1	65.3	63.4
2	RTFOT	60	G*, Pa	23	49	104	222	475	993	2054	4190	8431	16590
			d	91.2	91.3	89.4	88.3	87.5	86.1	84.7	83.4	82.0	80.7
		25	G*, Pa	10510	20410	38760	73060	134900	245500	441900	785200	1374000	2346000
			d	78.1	76.4	74.7	73.0	71.6	70.0	68.4	66.9	65.2	63.3
3	RTFOT	60	G*, Pa	22	50	105	225	476	998	2063	4203	8447	16600
			d	88.3	89.2	89.0	88.4	87.3	86.0	84.7	83.3	81.9	80.6
		25	G*, Pa	10290	19940	37690	70690	131900	238700	429900	764300	1335000	2276000
			d	78.5	76.2	74.2	72.6	71.4	69.8	68.4	66.9	65.1	63.2
1	RTFOT/PAV	60	G*, Pa	106	210	436	895	1809	3618	7105	13700	26020	48500
			d	82.5	84.6	84.5	83.6	82.2	80.4	78.5	76.7	75.0	73.5
		25	G*, Pa	52220	92570	162300	280200	478500	804100	1334000	2186000	3513000	5521000
			d	69.8	66.8	65.1	63.9	62.0	60.6	58.7	56.9	54.9	53.0
2	RTFOT/PAV	60	G*, Pa	89	192	400	831	1693	3421	6758	13070	24880	46500
			d	88.7	87.8	85.8	84.8	83.2	80.7	78.9	77.0	75.3	73.8
		25	G*, Pa	50730	87900	154200	265800	454800	766100	1272000	2085000	3349000	5274000
			d	68.6	66.8	65.1	63.5	62.0	60.3	58.7	56.9	55.0	53.0
3	RTFOT/PAV	60	G*, Pa	89	193	413	855	1742	3507	6919	13400	25500	47630
			d	89.5	87.2	86.0	84.9	82.9	80.9	78.9	77.0	75.3	73.7
		25	G*, Pa	46740	82460	145500	249200	424300	712400	1180000	1925000	3090000	4853000
			d	68.4	66.3	64.9	63.2	61.5	60.0	58.3	56.6	54.8	52.7
1	RTFOT/LTSAFT	60	G*, Pa	81	174	367	773	1581	3201	6356	12380	23730	44580
			d	88.0	88.6	87.3	85.4	83.5	81.6	79.6	77.7	76.0	74.5
		25	G*, Pa	47110	83880	147000	256900	436800	741400	1235000	2026000	3268000	5155000
			d	69.6	67.2	65.8	63.9	62.3	60.7	58.9	57.2	55.2	53.2
2	RTFOT/LTSAFT	60	G*, Pa	86	175	366	763	1546	3121	6187	12030	23020	43240
			d	88.3	86.7	85.3	83.7	82.8	81.2	79.3	77.6	75.8	74.3
		25	G*, Pa	40900	73260	129300	222900	382100	643800	1070000	1754000	2825000	4460000
			d	69.2	67.1	65.3	63.9	62.2	60.7	58.9	57.1	55.3	53.3
3	RTFOT/LTSAFT	60	G*, Pa	75	160	340	705	1459	2953	5861	11480	22040	41500
			d	88.5	86.8	86.9	85.2	83.7	81.8	79.9	78.0	76.2	74.7
		25	G*, Pa	52670	93670	164600	285500	486900	814000	1334000	2134000	3337000	4947000
			d	69.3	67.7	66.0	64.6	62.7	61.4	60.1	58.9	57.7	56.8

Table 14. DSR Frequency Sweep Data for the PG 82-22 Binder.

Replicate	Condition	Temp, C	Property	Freq.(rad/s)									
				0.10	0.22	0.46	1.00	2.15	4.64	10.00	21.54	46.41	100.00
1	RTFOT	60	G*, Pa	1036	1709	2788	4511	7375	12060	19830	32900	55120	93140
			d	58.2	58.1	57.8	57.8	58.0	58.5	59.3	60.4	61.5	62.7
		25	G*, Pa	103300	171300	285300	471600	782100	1282000	2078000	3317000	5206000	7920000
			d	58.7	59.0	59.2	59.1	58.4	57.7	56.5	55.1	53.5	51.7
2	RTFOT	60	G*, Pa	1036	1709	2788	4511	7375	12060	19830	32900	55120	93140
			d	58.2	58.1	57.8	57.8	58.0	58.5	59.3	60.4	61.5	62.7
		25	G*, Pa	89360	148800	249500	411100	681000	1117000	1811000	2889000	4517000	6839000
			d	59.0	59.2	59.1	59.1	58.4	57.6	56.4	55.1	53.5	51.8
3	RTFOT	60	G*, Pa	975	1595	2637	4278	7032	11520	18970	31530	52860	89420
			d	59.2	58.8	58.1	58.2	58.2	58.8	59.6	60.5	61.7	62.8
		25	G*, Pa	104400	172000	287500	477600	791800	1301000	2111000	3378000	5308000	8098000
			d	59.1	59.6	59.3	59.2	58.5	57.7	56.5	55.1	53.4	51.6
1	RTFOT/PAV	60	G*, Pa	3614	5581	8680	13420	20920	32780	51730	82590	133500	217700
			d	51.7	51.7	52.0	52.3	53.0	53.7	54.7	55.8	56.9	57.7
		25	G*, Pa	357500	568000	902300	1410000	2184000	3334000	5018000	7451000	10890000	15620000
			d	54.0	53.5	52.7	51.6	50.3	48.9	47.4	45.7	44.0	42.1
2	RTFOT/PAV	60	G*, Pa	4041	6203	9629	15010	23330	36460	57510	91830	148500	242400
			d	51.7	51.7	52.4	52.1	52.9	53.6	54.7	55.7	56.9	57.6
		25	G*, Pa	378700	602300	941600	1471000	2255000	3423000	5136000	7597000	11070000	15820000
			d	54.1	53.0	52.3	51.2	49.9	48.6	47.2	45.6	43.9	42.1
3	RTFOT/PAV	60	G*, Pa	4395	6739	10420	15990	24900	38920	61370	97710	157300	255700
			d	51.6	51.2	51.4	52.3	52.5	53.4	54.4	55.5	56.6	57.2
		25	G*, Pa	409200	639000	998000	1554000	2374000	3591000	5358000	7888000	11440000	16290000
			d	53.2	52.4	52.3	50.4	49.3	47.9	46.4	44.7	43.1	41.2
1	RTFOT/LTSAFT	60	G*, Pa	5248	8124	12570	19410	30210	47150	74360	118300	190600	309100
			d	52.3	51.9	51.7	52.2	52.7	53.4	54.4	55.4	56.2	56.7
		25	G*, Pa	439100	704900	1098000	1707000	2586000	3919000	5827000	8547000	12350000	17500000
			d	54.1	52.7	52.2	50.4	48.7	47.6	46.0	44.4	42.6	40.7
2	RTFOT/LTSAFT	60	G*, Pa	4157	6435	10040	15570	24410	38400	60990	97320	157400	256900
			d	52.9	52.9	52.5	52.9	53.2	54.1	55.0	56.0	56.9	57.5
		25	G*, Pa	491300	776300	1208000	1835000	2783000	4148000	6110000	8848000	12630000	17710000
			d	53.3	52.2	50.4	49.3	47.7	46.2	44.6	43.0	41.3	39.4
3	RTFOT/LTSAFT	60	G*, Pa	3951	6112	9533	15030	23530	37100	58910	94480	153300	251300
			d	53.0	53.0	53.6	53.0	53.6	54.3	55.4	56.4	57.2	57.9
		25	G*, Pa	435200	702200	1098000	1717000	2629000	3989000	5960000	8772000	12720000	18090000
			d	54.2	53.2	52.8	51.0	49.7	48.1	46.5	44.8	43.0	41.0

Table 15. BBR Data at –12 °C for PG 58-28 Binder.

Replicate	Beam	Time, s	RTFO		RTFO/PAV		RTFO/LTSAFT	
			S, MPa	m	S, MPa	m	S, MPa	m
1	1	8	114	0.438	178	0.365	164	0.358
		15	85.0	0.472	140	0.388	129	0.386
		30	60.7	0.510	106	0.414	97.8	0.416
		60	42.2	0.548	79.1	0.440	72.7	0.447
		120	28.4	0.585	57.7	0.466	52.8	0.478
		240	18.7	0.623	41.4	0.492	37.4	0.508
1	2	8	114	0.444	166	0.358	184	0.369
		15	85.6	0.476	132	0.383	145	0.396
		30	60.8	0.512	99.7	0.412	109	0.427
		60	42.1	0.547	74.4	0.440	80.3	0.457
		120	28.5	0.583	54.4	0.468	57.8	0.488
		240	18.8	0.618	38.8	0.497	40.7	0.518
2	1	8	118	0.440	158	0.336	177	0.356
		15	88.5	0.472	127	0.362	140	0.381
		30	63.1	0.507	97.6	0.391	106	0.409
		60	43.9	0.542	73.6	0.420	79.5	0.436
		120	29.8	0.577	54.6	0.448	58.2	0.464
		240	19.7	0.612	39.6	0.477	41.7	0.492
2	2	8	114	0.428	157	0.348	179	0.357
		15	86.5	0.459	125	0.371	142	0.380
		30	62.2	0.494	95.8	0.395	108	0.406
		60	43.4	0.529	72.5	0.420	80.8	0.432
		120	29.8	0.565	53.8	0.444	59.5	0.458
		240	19.9	0.600	39	0.469	42.8	0.483
3	1	8	117	0.434	160	0.346	169	0.358
		15	88.0	0.469	127	0.371	134	0.384
		30	62.7	0.508	97.6	0.399	102	0.414
		60	43.7	0.546	73.5	0.426	75.4	0.443
		120	29.6	0.585	54.1	0.454	54.9	0.473
		240	19.4	0.624	39.1	0.482	39.2	0.502
3	2	8	114	0.443	180	0.353	165	0.357
		15	85.8	0.472	142	0.379	130	0.383
		30	61.1	0.505	109	0.409	99.1	0.412
		60	42.5	0.537	80.9	0.438	73.8	0.441
		120	28.9	0.569	59.1	0.468	53.8	0.471
		240	19.4	0.601	42.3	0.497	38.4	0.500

Table 16. BBR Data at –12 °C for PG 82-22 Binder.

Replicate	Beam	Time, s	RTFO		RTFO/PAV		RTFO/LTSAFT	
			S, MPa	m	S, MPa	m	S, MPa	m
1	1	8	254	0.318	377	0.259	336	0.256
		15	206	0.345	318	0.283	284	0.281
		30	161	0.375	259	0.309	232	0.308
		60	123	0.405	207	0.336	185	0.335
		120	91.7	0.435	163	0.362	146	0.362
		240	66.9	0.466	125	0.389	112	0.389
1	2	8	260	0.310	362	0.258	342	0.250
		15	212	0.341	305	0.281	289	0.274
		30	165	0.376	249	0.306	237	0.300
		60	126	0.411	200	0.332	191	0.326
		120	93.4	0.446	157	0.357	151	0.353
		240	67.7	0.481	122	0.382	117	0.379
2	1	8	225	0.295	334	0.255	380	0.248
		15	185	0.327	282	0.277	323	0.272
		30	145	0.363	232	0.301	265	0.298
		60	112	0.399	186	0.326	214	0.324
		120	83.6	0.435	148	0.350	169	0.350
		240	61.1	0.471	115	0.375	131	0.376
2	2	8	241	0.323	346	0.262	404	0.246
		15	195	0.351	292	0.283	343	0.268
		30	151	0.382	238	0.307	283	0.292
		60	115	0.412	191	0.330	229	0.316
		120	85.3	0.443	150	0.354	183	0.340
		240	62.0	0.474	117	0.378	143	0.364
3	1	8	258	0.315	326	0.257	376	0.250
		15	209	0.347	275	0.282	318	0.274
		30	162	0.382	224	0.309	261	0.300
		60	124	0.416	180	0.337	210	0.326
		120	91.3	0.451	141	0.364	166	0.353
		240	65.9	0.486	108	0.392	129	0.379
3	2	8	244	0.325	328	0.274	360	0.257
		15	197	0.354	275	0.297	303	0.278
		30	152	0.386	221	0.322	248	0.303
		60	115	0.418	176	0.347	200	0.327
		120	85.5	0.449	137	0.372	158	0.351
		240	61.9	0.481	105	0.398	123	0.375